Propulsion and Power Research 2023;12(1):153–165

http://ppr.buaa.edu.cn/

Propulsion and Power Research

www.sciencedirect.com

ORIGINAL ARTICLE

Insight into the relationship between non-linear mixed convection and thermal radiation: The case of Newtonian fluid flow due to non-linear stretching

Amit Kumar Pandey[a], **Krishnendu Bhattacharyya**[a,*], **Anil Kumar Gautam**[a], **Sohita Rajput**[a], **Mani Shankar Mandal**[b], **Ali J. Chamkha**[c], **Dhananjay Yadav**[d]

[a]*Department of Mathematics, Institute of Science, Banaras Hindu University, Varanasi-221005, Uttar Pradesh, India*
[b]*Department of Mathematics, Government General Degree College, Kalna—I, Burdwan-713405, West Bengal, India*
[c]*Faculty of Engineering, Kuwait College of Science and Technology, Doha District, Kuwait*
[d]*Department of Mathematical and Physical Sciences, University of Nizwa, Oman*

Received 17 September 2021; accepted 18 October 2022
Available online 20 December 2022

KEYWORDS
Non-linear mixed convection;
Non-linear thermal radiation;
Non-linear stretching sheet;
Newtonian fluid

Abstract The current research focuses the light on the characterization of buoyancy-driven non-linear mixed convection and non-linear radiation in a Newtonian flow over a non-linearly stretching vertical sheet, and this type of flow has useful applications in many industrial processes, such as the paper and pulp industry, polymer industry, electronic device cooling, solar collectors, gas turbine plants, and nuclear power. Using appropriate transformations, governing PDEs for non-linear mixed convection are reduced to higher-order non-linear ODEs and those are numerically solved. Along with tabular presentations of computed results, the graphical representations are generated to elucidate the effects of involved parameters on convection transport properties and their inter-relations. It demonstrates that flow velocity increases near the surface and decreases away from the surface as the non-linear convection parameter

*Corresponding author.
E-mail addresses: krish.math@yahoo.com, krishmath@bhu.ac.in (Krishnendu Bhattacharyya).
Peer review under responsibility of Propulsion and Power Research.

Production and Hosting by Elsevier on behalf of KeAi

https://doi.org/10.1016/j.jppr.2022.11.002

increases. Furthermore, increments in the thermal buoyancy, temperature ratio and non-linear radiation parameters result in the boost of velocity. The temperature decreases as linear and non-linear buoyancy-related parameters (non-linear convection and thermal buoyancy parameters) are of higher levels. In contrast, the temperature rises with two non-linear thermal radiation-related parameters (thermal ratio and non-linear radiation parameters). For greater values of the non-linear stretching related parameter, a lower velocity and a higher temperature are witnessed. The non-linear convection, thermal buoyancy, thermal ratio and non-linear radiation parameters contribute toward the reduction of the magnitude of surface-drag force and growth of the surface cooling rate. But, with the non-linearity in surface stretching there are significant percentage hikes of surface-drag force magnitude and surface cooling rate.

Nomenclature

A_2	non-linear convection parameter
C_f	skin-friction coefficient
f	dimensionless stream function
g	acceleration due to gravity
Gr_x	Grashof number
k^*	absorption constant
n	non-linear stretching parameter
N_r	non-linear radiation parameter
Nu	Nusselt number
Pr	Prandtl number
q_w	surface heat flux
q_r	radiative heat flux
Re_x	Reynolds number
T_w	temperature at sheet
T_∞	ambient temperature
U_w	stretching velocity
u, v	velocity component in the x- and y-direction

Greek symbols

Ω_1, Ω_2	coefficients of thermal linear and non-linear expansions
η	a dimensionless variable
θ_w	temperature ratio parameter
λ	local thermal buoyancy parameter
μ	dynamic viscosity
υ	kinematic viscosity
ψ	dimensionless stream function
τ_w	surface shear stress
ρ	density
ρc_p	heat capacity
σ^*	Stefan-Boltzman constant
κ	thermal conductivity

Subscripts

w	initial conditions at the surface of sheet
∞	conditions in the free stream

Abbreviations

IVP	initial value problem
MHD	magnetohydrodynamic
ODEs	ordinary differential equations
OHAM	optimal homotopy asymptotic method
PDEs	partial differential equations

1. Introduction

Mixed convection flow is caused by a combination of two existing convection flow mechanisms, namely, forced flow of convection and free flow of convection, and it is commonly seen in various transport processes in engineering and industries. These flow patterns are caused by a mechanism of external and volumetric internal forces, and they are important in domains such as atmospheric boundary-layer flows, solar collectors, various electronic equipment, nuclear reactors, and heat exchangers. When buoyancy force is significant in forced convection and forced flow is prominent in free convection, mixed convection occurs. The interaction between forced and free convection becomes apparent when the velocity of forced flow is low and/or the temperature difference is large. Mixed convection flow is critical to a variety of industrial problems, including, pulp and paper production, rubber and polymer sheet manufacturing and extraction, wire manufacturing, and glass-fiber production. Other typical applications of mixed convection may be found in steel extrusion, liquid films associated with the condensation process, ample metallic plate cooling in a bath, liquid films in the aerodynamics, and heat treatment mechanism of the material, which is traveling between a set of feed, conveyor belts, wind-up rolls, etc. It is evident that this flow type has an impact in the area of thermal manufacturing processes, and thus it is critical in achieving temperature uniformity.

The radiative heat transfer flow is acknowledged as an essential aspect for the design of many types of equipment with high reliability, such as nuclear & gas turbine plants and different propulsion systems for various aviation and space technology machines like satellites, missiles, aircraft, and other space vehicles. Radiative heat transfer, like mixed convection, is also essential in the many manufacturing industries. Thermal radiation has a significant impact on heat transfer in polymer processing. The quality of manufactured polymer is primarily determined by heat controlling factors up to a specific degree. Similarly, the design and development of some advanced energy convection processes and systems (which operate at a higher temperature), the effect and outcome of thermal radiation in a flow have a significant influence on the heat transfer process. Thermal radiation that occurs within defined procedures and systems is typically the result of emission caused by the interaction between the hot walls of the system and working fluid, which is under consideration. The thermal radiation effect becomes essential when variability between the wall surface and ambient temperatures is significantly high. Considering all these aspects and established observations, it is pretty clear that thermal radiation is one of the crucial parameters for controlling heat transfer in various processes. Another significant part of acknowledging thermal radiation is to enhance the cooling liquid's thermal diffusivity in the problems related to the stretching sheet. As a result, it can be concluded that understanding radiation heat transfer in the aforementioned process/system will help in developing a desirable product with appropriate characteristics.

The heat transfer phenomenon, which is greatly influenced by thermal radiation is widely applicable in technology-related processes, such as various propulsion devices, gas turbine plants, and nuclear power. Radiation (linear) effects on heat transfer in Blasius flow were examined by Mabood et al. [1] using the optimal homotopy asymptotic method (OHAM). Thermal radiation (linear) effect on Blasius flow with heat transfer with Merkin boundary conditions was scrutinized by Khan et al. [2]. However, when temperature differences are very high, linear radiation is not a legal assumption. In this framework, Hayat et al. [3] investigated the effects of non-linear thermal radiation and external uniform magnetic field on the 3D couple stress nanofluids flow with Brownian motion and thermophoresis. Shehzad et al. [4] discussed relevant characters of Brownian movement and thermophoresis in the 3D flow of Jeffrey nanofluid possessing the magnetohydrodynamic (MHD) properties with non-linear thermal radiation. Non-linear thermal radiation effect on double-diffusive free convection flow of viscoelastic nanofluid past an expanding sheet was discussed by Kumar et al. [5]. Boundary layer viscoelastic flow with heat transfer past expanding sheet with non-linear thermal radiation and induced magnetic field had been conveyed by Animasaun et al. [6]. Hayat et al. [7] examined MHD 3D nanoliquid flow with non-linear thermal radiation and velocity slip. Nandeppanavar et al. [8] investigated the effect of nonlinear thermal radiation on the stagnation point flow of a moving vertical plate in double-diffusive free convection and they explored that as the buoyancy ratio parameter and the parametric value of the Rayleigh number increase, velocity decreases. Ahmad et al. [9] investigated heat transfer for MHD Maxwell fluid in porous medium considering variable thermal conditions. Mahanthesh et al. [10] considered non-linear radiation, melting, and viscous effects on mixed-convectional nanoliquid flow. Optimal homotopy analysis of micropolar flow with thermal stratification and non-linear thermal radiation was reported by Koriko et al. [11]. Khan et al. [12] and Song et al. [13] discussed the influence of non-linear thermal radiation on bio-convective micropolar nanofluid flow over a rotating disk with slip and without slip. Waqas et al. [14] explored the useful characteristics of non-linear thermal radiation along with activation energy and melting process in a time-dependent Falkner-Skan flow. Recently, Bilal et al. [15] reported the role of nonlinear thermal radiation in the optimization of entropy for MHD Williamson nanofluid flow in non-Darcy porous medium and also obtained solutions by homotopy analysis method (HAM).

Many investigated mixed convection problems in the literature are based on linear mixed convection, but nonlinearities should be included in many phenomena (e.g., combustion, electronic device cooling, solar collectors, reactor safety areas) due to their significant effect on the flow and thermal transport. Goren [16] considered quadratic density temperature variation, i.e., $(T - T_\infty)^2$ rather than linear density temperature variation. Ali et al. [17] explored the improved thermal transportation for bio-convection and mixed convection of Casson nanofluid flow in the stagnation area of a rotating sphere. They concluded that for increased buoyancy and rotation the magnitude of the Nusselt number rises, but it decreases when compared to Brownian motion, bio convection, and Rayleigh number. Mahanthesh et al. [18] studied 3D non-linear convection of a non-Newtonian nanofluid having solar radiation. They have established that for solar radiation, the temperature is more robust. Non-linear convection impact on MHD thixotropic fluid flow was reported by Hayat et al. [19]. Whereas non-linear convection for the stratified flow of third-grade fluid was studied by Waqas et al. [20]. Gireesha et al. [21] considered the non-linear convective flow of nano liquid with variable viscosity and exponential heat source. After that, Bandaru et al. [22] explored a heat and mass transfer problem with non-linear mixed convection in a rotating cone. Unsteady non-linear mixed convection flow with velocity slip and activation energy is numerically analyzed by Uddin et al. [23]. Mahanthesh et al. [24] reported the quadratic convections of Casson and Carreau dusty fluids on the stretchable surface taking the effect of magnetic dipole and non-linear thermal radiation. Kunnegowda et al. [25] conferred induced magnetic field effect on MHD quadratic convective Casson fluid flow in a microchannel using HPM. Alsaedi et al. [26] explained non-linear mixed convection on stretchable surfaces. Recently, Hong et al. [27] explored stagnation point flow past a cylinder taking non-linear mixed convection. Some articles [28−32] are available in literature exploring many important aspects of the non-linearity of mixed convection and its impacts on flow and heat transfer properties.

The analysis of 2D flow and heat transfer over a non-linear stretching surface is essential, as it has various useful applications in earth sciences, particularly in geothermal energy extraction and underground storage systems. Furthermore, during the cooling process, the speed and temperature of the stretched surface play an important role in so many existing manufacturing processes. In the present situation, it is established and well known in the scientific community that stretching is not always linear. Several researchers have analyzed different transport mechanisms, such as momentum, heat, and mass transports over non-linear stretching surfaces. Cortell [33] discussed flow induced by the non-linear expansion of the sheet. Rana and Bhargava [34] studied laminar steady flow (of nanofluid), which has been resulted from the non-linear expansion of flat surface. Pal and Mandal [35] procured numerical solutions by shooting method with 5th order Runge-Kutta-Fehlberg (RKF) technique for MHD flow of a convective nanofluid electrically conducting in nature, where flow is induced by a non-linearly stretching/shrinking vertical sheet with thermal radiation and Ohmic heating. Gangadhar et al. [36] used a numerical technique to calculate the Casson fluid solutions for a nonlinear stretching sheet with mixed convection and discovered that the nonlinearity in stretching causes contraction of the velocity field. Turkyilmazoglu [37] completed an analytical study on MHD slip flow with thermal transport characteristics over a continuous stretching sheet. He looked into the structure of solutions and calculated the thresholds of multiple solutions. Fenuga et al. [38] studied the impacts of radiation and Eckert number on a nonlinear vertical stretching sheet having an MHD flow with heat transfer near a stagnation-point region. They came to the conclusion that as radiation, Eckert number, and flow temperature increase, the heat transfer rate at the surface decreases. Turkyilmazoglu [39] also described classical Jeffery-Hamel flow in convergent/divergent channels when the channel walls are stretchable or shrinkable. Heat transfer in non-Newtonian (power-law) flow over a non-linear expanding surface was examined by Prasad et al. [40] and Mahmoud et al. [41] also studied power-law fluid flow on the non-linear expanding sheet with heat generation phenomenon. Similarly, heat transfer in a non-Newtonian fluid flow over a non-linear expanding permeable surface was illustrated by Jothimani and Vidhya [42]. Khan and Hashim [43] described Carreau fluid flow on a non-linear expanding sheet. In the past few years, numerous similarity solutions for some problems involving stretching/shrinking sheet have been considered on stretching and shrinking sheets by various researchers. Out of which, in some cases, multiple solutions exist, and it is because of involved parameters, such as mixed convection, unsteady, suction parameters. Those works show that the probability of multiple similarity solutions for the flow past shrinking sheet is more significant than that for stretching sheet. It is also noted from the previously published literature that due to the existence of non-linearity in flow governing equations, non-uniqueness of the solution may occur. For non-Newtonian fluid models, flow contains non-linear terms, which may lead to many interesting properties. Hamid et al. [44] inspected the heat-mass transport on MHD flow of unsteady Williamson nanofluid with source/sink in a permeable channel. Buoyancy effects and thermal radiation are also taken into consideration.

Motivated by the regular occurrence of mixed convection flow in many engineering and industrial processes, as well as the importance of radiative heat transfer in high-temperature problems and their applications, this paper considers Newtonian flow due to non-linear vertical stretching sheet with an insight of non-linear mixed convection phenomenon and non-linear thermal radiation. The primary goal of the investigation is to examine the combined effects of non-linear mixed convection and non-linear thermal radiation on the flow field and the relationship between these phenomena. As per our knowledge, this problem has not yet been investigated. Non-linearity in convective flow is extremely important in modern-day's context. Because of the significant effect of non-linear mixed convection on flow and thermal transport, quadratic mixed convectional Newtonian flow over a non-linearly stretching vertical sheet has many engineering applications, including chemical and food processing, polymer industry, propulsion devices, gas turbine plants, electronic device cooling, and nuclear power. The novelty of the current analysis lies in the study of Newtonian flow due to non-linear vertical stretching sheet with an understanding of non-linear mixed convection phenomenon and non-linear thermal radiation, which is motivated by the wide range of applications of Newtonian flow over a non-linear stretching sheet. The governing mixed convectional PDEs are transformed into ODEs. The solutions of those are obtained by the well-known and very effective technique "bvp4c", a package of MATLAB with necessary validation of results by comparison with available data in the literature to confirm the accurateness. Also, the efficiency and correctness of the numerical scheme are well-established by several published articles. Later, essential effects of non-linearity are explored and analyzed through graphical and tabular modes of presentations of the computed results.

2. Mathematical formulation

Consider the steady-state interaction between non-linear mixed convection and non-linear thermal radiation in a flow due to non-linear stretching vertical surface. The x-axis considers along expanding surface, whereas the y-axis is considered upright to it. All fluid properties are assumed to remain constant. The fluid is taken as incompressible and flow is considered to be 2-dimensional. Taking into account the boundary layer and Boussinesq approximations, the basic equations for mass, momentum, and energy conservations are specified as follows [26,45–47]:

$$\frac{\partial u}{\partial x}+\frac{\partial v}{\partial y}=0 \tag{1}$$

$$u\frac{\partial u}{\partial x}+v\frac{\partial u}{\partial y}=\upsilon\frac{\partial^2 u}{\partial y^2}+g\left[\Omega_1(T-T_\infty)+\Omega_2(T-T_\infty)^2\right] \tag{2}$$

$$u\frac{\partial T}{\partial x}+v\frac{\partial T}{\partial y}=\alpha\frac{\partial^2 T}{\partial y^2}-\frac{1}{\rho c_p}\frac{\partial q_r}{\partial y} \tag{3}$$

with conditions [43]:

$$\left.\begin{array}{l} u=U_w=bx^n,\;\; v=0,\;\; T=T_w \text{ at } y=0,\\ u\to 0,\;\; T\to T_\infty \text{ as } y\to\infty, \end{array}\right\} \tag{4}$$

where u and v are the velocity components along x- and y-directions, respectively, T is the temperature, $\upsilon=\mu/\rho$ is the kinematic viscosity of nanofluid, $\alpha=\kappa/(\rho c_p)$ is the thermal diffusivity, Ω_1 and Ω_2 denote the coefficients of thermal linear and non-linear expansions, U_w is the stretching velocity with $b(>0)$ being a constant and n being the non-linear stretching parameter, T_w and T_∞ are constant temperatures at the sheet and in free stream with $T_w > T_\infty$ and μ, ρ, κ are the viscosity, density, thermal conductivity, respectively. Also, a diagram with geometry of problem is plotted in Figure 1.

Here, radiative heat flux q_r is defined as [24] $q_r=-\frac{4\sigma^*}{3k^*}\frac{\partial T^4}{\partial y}=-\frac{16\sigma^*}{3k^*}T^3\frac{\partial T}{\partial y}$, where k^* and σ^* are the absorption coefficient and Stefan-Boltzman constant, respectively. So, Eq. (3) becomes

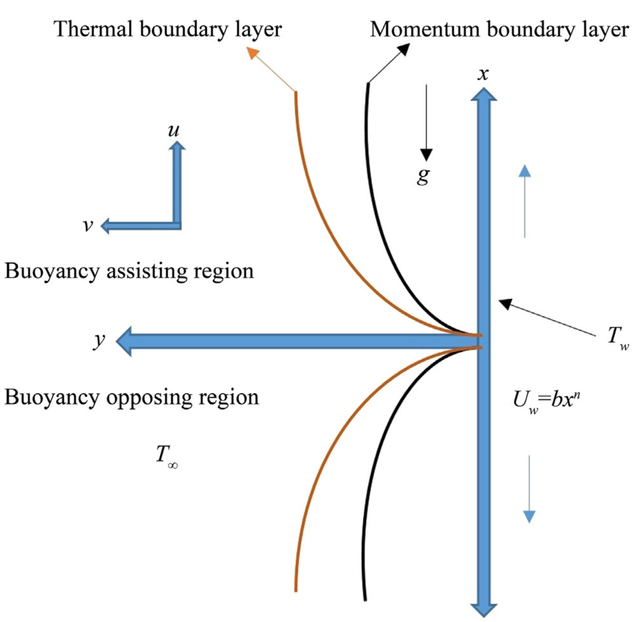

Figure 1 Physical sketch of the problem.

$$u\frac{\partial T}{\partial x}+v\frac{\partial T}{\partial y}=\alpha\frac{\partial^2 T}{\partial y^2}+\frac{16\sigma^*}{3\rho c_p k^*}\left[3T^2\left(\frac{\partial T}{\partial y}\right)^2+T^3\frac{\partial^2 T}{\partial y^2}\right] \tag{5}$$

In the above equations, the non-linear radiation terms in Eq. (5) and non-linear mixed convection term in Eq. (2) are two novel aspects of this study and their simultaneous impacts on velocity and temperature profiles due to non-linearly stretching sheet are equally crucial.

The following transformations are used [43]:

$$\left.\begin{array}{l} \psi(x,y)=\sqrt{\dfrac{2\upsilon b}{n+1}}x^{\frac{n+1}{2}}f(\eta),\;\; T=T_\infty[1+(\theta_w-1)\theta(\eta)],\\ \eta=y\sqrt{\dfrac{b(n+1)}{2\upsilon}}x^{\frac{n-1}{2}}, \end{array}\right\} \tag{6}$$

where ψ is the usual stream function ($u=\frac{\partial\psi}{\partial y}$ and $v=-\frac{\partial\psi}{\partial x}$), η is a dimensionless variable and $\theta_w=T_w/T_\infty$ is the temperature ratio parameter.

Using the transformation in Eq. (6), Eqs. (2) and (5) is transformed to

$$f'''+ff''-\frac{2n}{n+1}f'^2+\frac{2\lambda}{n+1}\theta[1+A_2\theta]=0 \tag{7}$$

$$\theta''+Nr\theta''[1+(\theta_w-1)\theta]^3+3Nr\theta'^2(\theta_w-1)[1+(\theta_w-1)\theta]^2+Prf\theta'=0 \tag{8}$$

with

$$f(0)=0,\;\; f'(0)=1,\;\; \theta(0)=1,\;\; f'(\infty)=0 \;\text{ and }\; \theta(\infty)=0 \tag{9}$$

where $\lambda=\frac{Gr_x}{Re_x^2}$ is the local thermal buoyancy parameter with $Gr_x=\frac{g\Omega_1(T_w-T_\infty)x^3}{\upsilon^2}$ being the Grashof number and $Re=\frac{U_w x}{\upsilon}$ being local Reynolds number, $A_2=\frac{\Omega_2(T_w-T_\infty)}{\Omega_1}$ is the non-linear convection parameter, $Nr=\frac{16\sigma^* T_\infty{}^3}{3k^*\kappa}$ is non-linear radiation parameter, and $Pr=\frac{\upsilon}{\alpha}$ is the Prandtl number. All the parameters above are dimensionless.

Quantities for physical interest, the local skin-friction coefficient, and the local Nusselt number are presented as [8]:

$$C_f=\frac{(\tau_w)_{y=0}}{\rho U_w^2} \quad\text{and}\quad Nu=\frac{x(q_w)_{y=0}}{\kappa(T_w-T_\infty)} \tag{10}$$

where $\tau_w=\mu\left(\frac{\partial u}{\partial y}\right)$ and $q_w=-\kappa\left(\frac{\partial T}{\partial y}\right)+(q_r)$.

So, above quantities reduce to

$$\left.\begin{array}{l} Re^{1/2}C_f=\sqrt{\dfrac{n+1}{2}}f''(0),\\ Re^{-1/2}Nu=-\sqrt{\dfrac{n+1}{2}}(1+Nr\theta_w{}^3)\theta'(0). \end{array}\right\} \tag{11}$$

3. Solution methodology

The resulting equations (7)-(8) with (9) are solved by MATLAB inbuilt function "bvp4c". For more details about this numerical approach, one can look into the book by Shampine et al. [48]. To solve the equations mentioned above using "bvp4c", we need to convert those into a set of first-order ODEs as given below:

$$y_1' = y_2,\ y_2' = y_3,\ y_3' = \frac{2n}{n+1}y_2^2 - \frac{2\lambda}{n+1}y_4[1 + A_2 y_4] - y_1 y_3 \tag{12}$$

$$y_4' = y_5,\ y_5' = \frac{-3Nry_5^2(\theta_w - 1)[1 + (\theta_w - 1)y_4]^2 - Pr\, y_1 y_5}{1 + Nr[1 + (\theta_w - 1)y_4]^3} \tag{13}$$

with

$$y_1(0) = 0, y_2(0) = 1, y_2(\infty) = 0, y_4(0) = 1 \quad \text{and} \quad y_4(\infty) = 0 \tag{14}$$

where $f(\eta) = y_1(\eta)$ and $\theta(\eta) = y_4(\eta)$.

The bvp4c is a finite-difference code that runs the three-stage Lobatoo IIIa formula, which is a collocation formula. The collocation polynomial provides a C^1-continuous solution with fourth-order accuracy uniformly across the integration interval.

Now to integrate the non-linear initial value problem (IVP) (12)−(14) using MATLAB inbuilt function "bvp4c", we have to assume the guess values for $y_3(0)$ and $y_5(0)$, which are required but not given and the infinite value of η in the boundary, i.e., $\eta \to \infty$ is required to be approximated to a suitable finite value, say, $\eta_\infty (= 10)$. The guess values are so chosen that the boundary conditions $y_2(\eta_\infty) = 0$ and $y_4(\eta_\infty) = 0$ satisfy asymptotically with desired accuracy level 10^{-5}. The working steps of the aforesaid solution method are presented by a flow chart in Figure 2 [49−51].

4. Description and discussion of obtained results

The solutions of the present work are computed for various values of local thermal buoyancy parameter λ, non-linear convection parameter A_2, non-linear stretching parameter n, Prandtl number Pr, temperature ratio parameter θ_w, and non-linear radiation parameter Nr. Graphical and tabular presentations of computed solutions are exhibited. If any of the parameters do not have a varying form, then the fixed values of those are taken as $\lambda = 0.2$, $A_2 = 0.5$, $n = 0.5$, $Pr = 3$, $Nr = 0.5$ and $\theta_w = 1.5$. To ensure the precision of the adopted numerical procedure, Table 1 and Table 2 illustrate comparisons of values of $-f''(0)$ and $-\theta'(0)$ with Cortell [33] and Khan and Hashim [43] for various values of n and there is a high level of agreement between

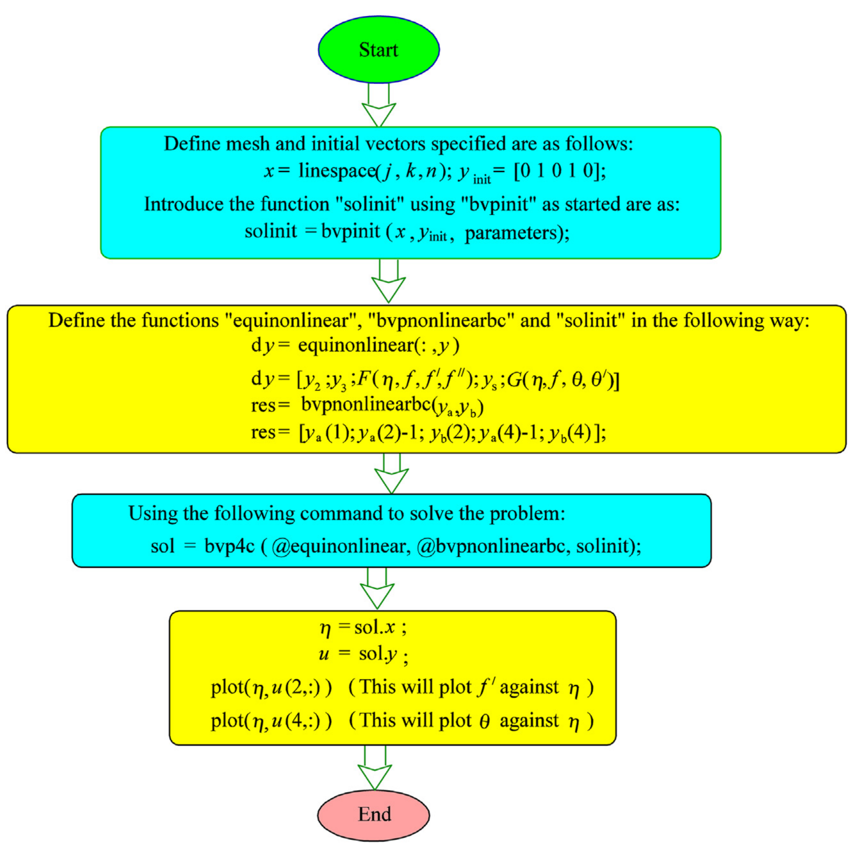

Figure 2 Flow chart of the solution methodology problem.

Table 1 The comparison of values of $-f''(0)$ for different n when $Pr = 1, Nr = 0, \theta_w = 1, \lambda = 0, A_2 = 0$.

n	Cortell [33]	Khan and Hashim [43]	Present result
0	0.627547	0.6275549	0.6275622
0.5	0.889477	0.889544	0.8895518
1	1.0	1.0	1.0000000
1.5	1.061587	1.061601	1.0616092
3	1.148588	1.148593	1.1486013
10	1.234875	1.234875	1.2348698

Table 2 The comparison of values of $-\theta'(0)$ for different n when $Pr = 1, Nr = 0, \theta_w = 1, \lambda = 0, A_2 = 0$.

n	Cortell [33]	Khan and Hashim [43]	Present result
0.2	0.610262	0.610202	0.6102157
0.5	0.595277	0.595201	0.5952206
1.5	0.574537	0.574730	0.5747719
3	0.564472	0.564662	0.5647180
10	0.554960	0.554951	0.5549513

them, indicating that they are correct. Also, to confirm the grid impendence of the adopted method, the values of $f'(\eta)$ and $\theta(\eta)$ are computed for two different grid sizes and are exhibited in Table 3. From those values, it is pretty clear that the obtained values are not dependent on the grid size.

Figure 3 portrays the contrasting effects of the non-linear convection parameter, A_2 on the velocity $f'(\eta)$. It is observed that velocity near the surface exhibits an increasing trend with A_2, whereas velocity away from the surface exhibits a decreasing trend. Since the temperature difference near the surface is greater, the second-order term due to thermal buoyancy has a stronger effect on velocity, and the effect fades as the temperature difference decreases towards the free stream. Also, as A_2 is proportional to the ratio of non-linear to linear thermal expansion coefficients, it should be varied in a non-negative manner, with zero representing linear convection. Furthermore, for greater values of A_2, the non-linear thermal expansion coefficient increases, which causes the improvement of the velocity near the considered sheet. Figure 4 explains the outcome of the non-linear convection parameter A_2 on temperature $\theta(\eta)$. It is detected that temperature falls when A_2 increases. For consideration of non-linear mixed convection along with linear, the cooling significantly enhances and consequently, diminution of temperature is witnessed.

Similarly, the relationship between velocity and λ can be visualized using Figure 5; which shows that with increasing

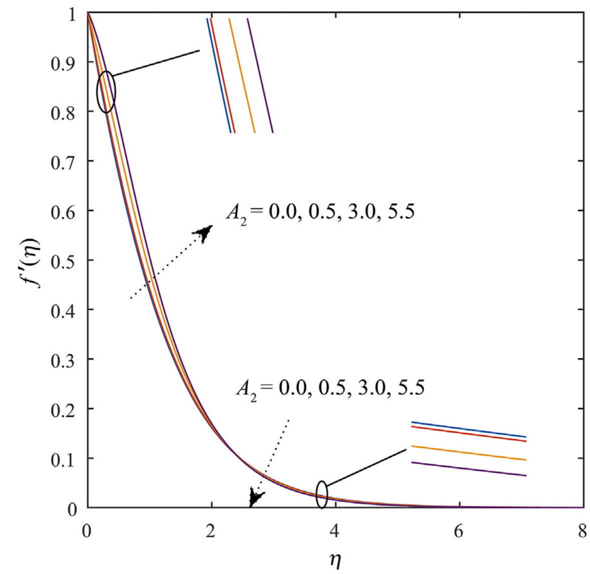

Figure 3 Effect of A_2 on $f'(\eta)$.

Table 3 The obtained values of $f'(\eta)$ and $\theta(\eta)$ for several η for different grid size.

	$f'(\eta)$		$\theta(\eta)$	
η	Grid size 0.01	Grid size 0.005	Grid size 0.01	Grid size 0.005
0	1.0000	1.0000	1.0000	1.0000
0.5	0.6821	0.6823	0.6691	0.6694
1	0.4400	0.4402	0.3657	0.3660
1.5	0.2712	0.2714	0.1639	0.1641
2	0.1620	0.1622	0.0636	0.0638
2.5	0.0948	0.0949	0.0227	0.0228
3	0.0547	0.0549	0.0077	0.0078
3.5	0.0314	0.0316	0.0026	0.0026
4	0.0170	0.0172	0.0008	0.0008
4.5	0.0096	0.0098	0.0003	0.0003
5	0.0054	0.0056	0.0001	0.0001
5.5	0.0030	0.0031	0.0000	0.0000
6	0.0016	0.0017	0.0000	0.0000
6.5	0.0008	0.0008	0.0000	0.0000
7	0.0004	0.0004	0.0000	0.0000
7.5	0.0001	0.0001	0.0000	0.0000
8	0.0000	0.0000	0.0000	0.0000

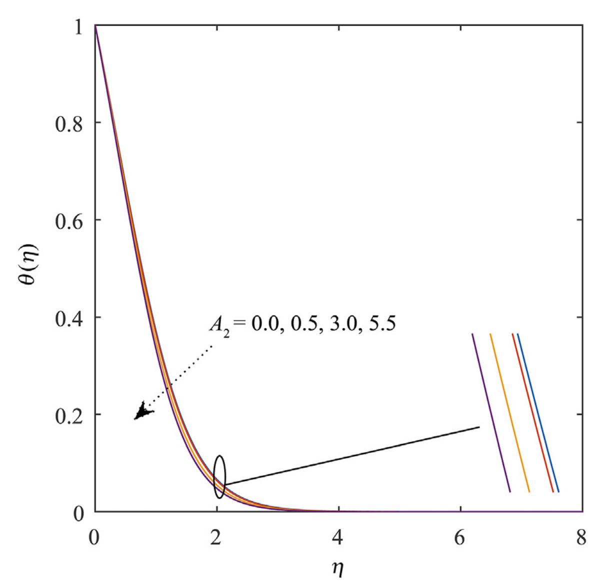

Figure 4 Effect of A_2 on $\theta(\eta)$.

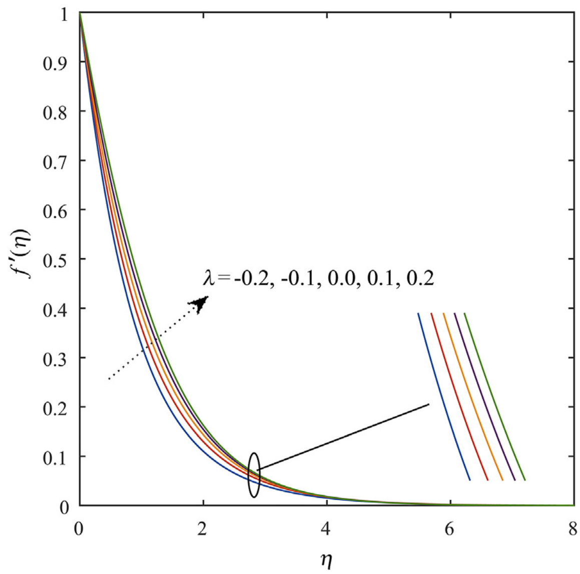

Figure 5 Effect of λ on $f'(\eta)$.

value of λ, velocity shows an increasing trend, i.e., for assisting flow ($\lambda > 0$) it rises and for opposing flows ($\lambda < 0$) it decreases. The reason for this lies in the fact that a favourable pressure gradient is induced for positive λ, which accelerates the motion, and for negative λ, a reverse case happens. For the opposing flows ($\lambda < 0$), the buoyancy effect is slightly more significant as compared to assisting flow ($\lambda > 0$). Figure 6 demonstrates the temperature $\theta(\eta)$ for various values of thermal buoyancy parameter. For assisting flow, the temperature profile decreases with λ and shows a vice-versa trend in case of opposing flow. This happens due to the usual linear mixed convection assumption and the two opposite buoyancy forces for it.

Non-linear stretching parameter's (n) impacts upon dimensionless velocity and temperature are demonstrated in Figures 7 and 8. It displays a fall velocity with increasing values of n and temperature exhibits a contrary nature. So, the increment of the parameter n leads to the decline of velocity. It can be observed that the large values of the stretching parameter n, thins the momentum boundary layer thickness. For non-linear stretching sheet case surface-drag and cooling rate increase which produces decreasing trends of velocity and temperature.

Figures 9–12 respectively depict the effect of non-linear radiation parameter Nr and temperature ratio parameter θ_w on the velocity $f'(\eta)$ and temperature $\theta(\eta)$. It is interestingly witnessed that velocity and temperature profiles show increasing trends with larger values of both Nr and θ_w. With an increase in the radiation parameter, more heat is transmitted to the fluid, resulting in a significant increase in temperature

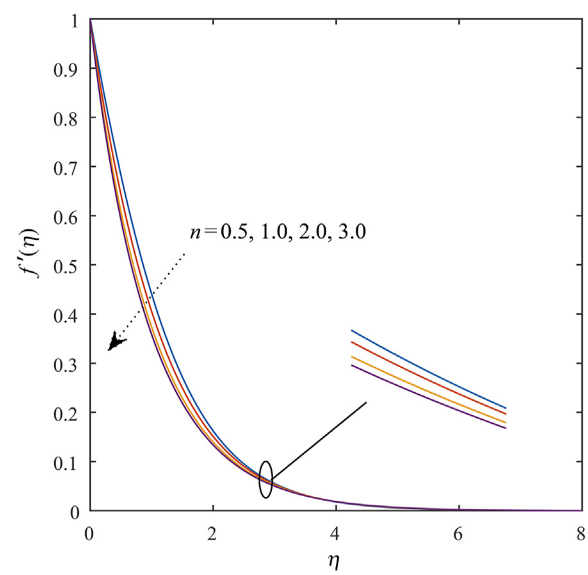

Figure 7 Effect of n on $f'(\eta)$.

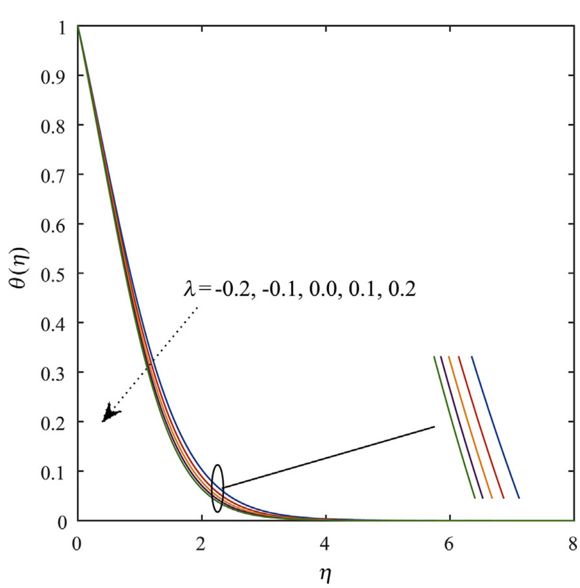

Figure 6 Effect of λ on $\theta(\eta)$.

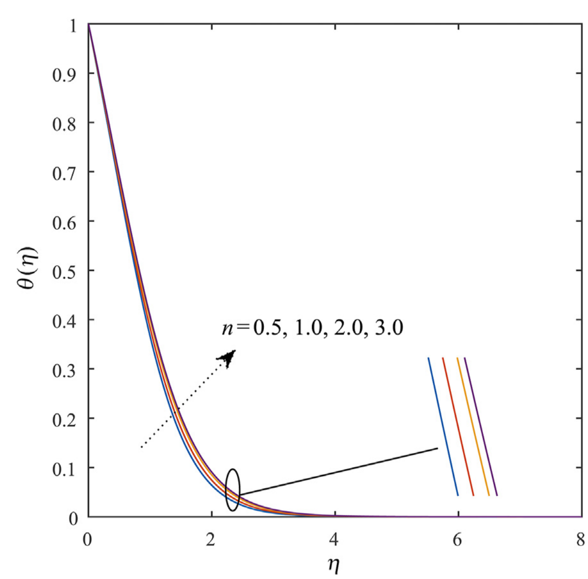

Figure 8 Effect of n on $\theta(\eta)$.

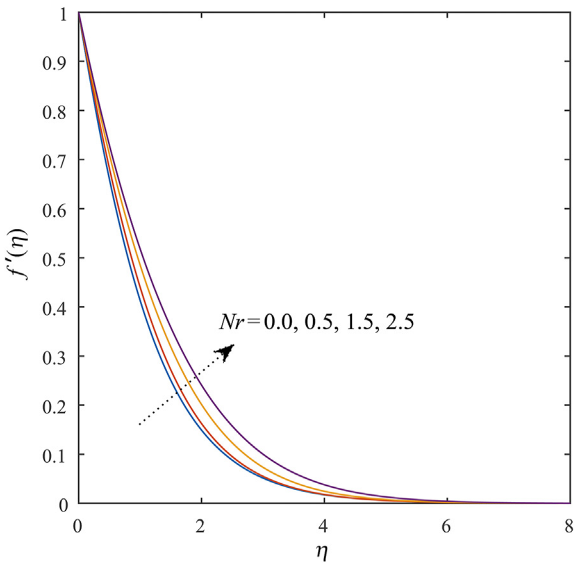

Figure 9 Effect of Nr on $f'(\eta)$.

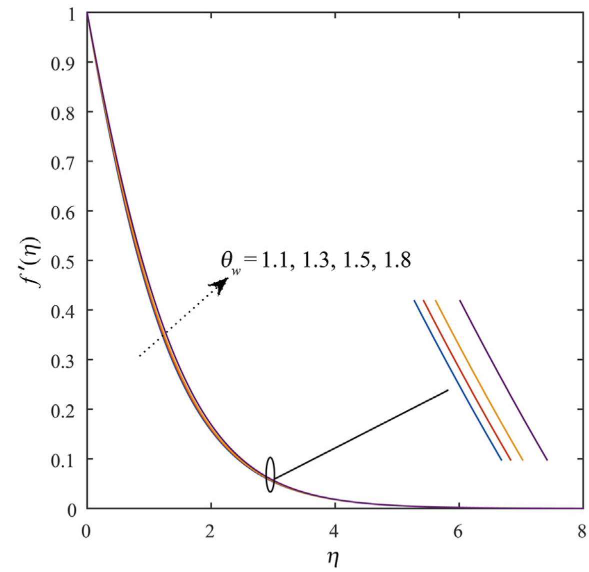

Figure 11 Effect of θ_w on $f'(\eta)$.

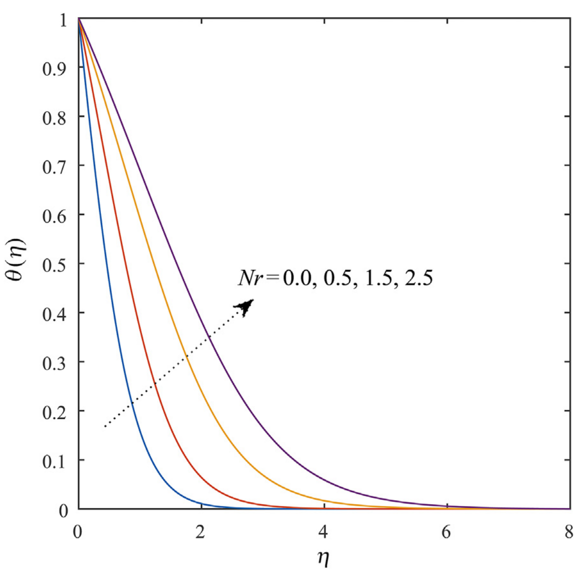

Figure 10 Effect of Nr on $\theta(\eta)$.

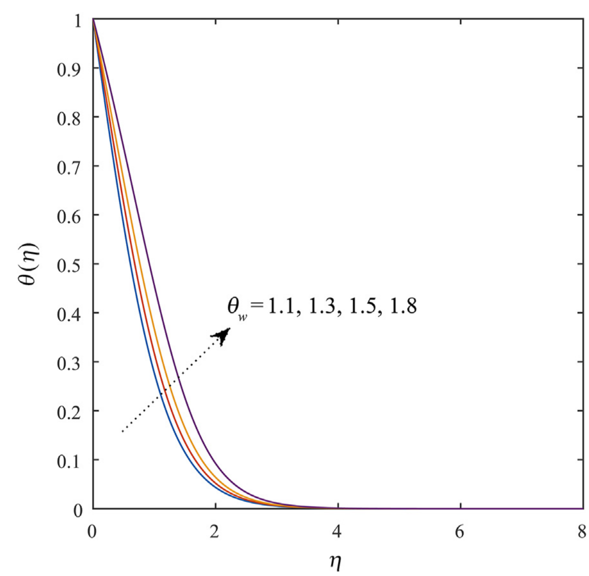

Figure 12 Effect of θ_w on $\theta(\eta)$.

inside the boundary layer and, as a result, an increase in thermal boundary layer thickness. The non-linear thermal radiation in the energy equation also results in an augmentation of fluid temperature. The temperature ratio parameter, θ_w is equally important in the non-linearity of thermal radiation and its unit value provides the linear thermal radiation case, so it is taken as greater than one. Furthermore, it is discovered that increasing the temperature ratio parameter results in an increase in both the temperature and thickness of the thermal boundary layer. If θ_w is not unity, then 2nd order radiation becomes active in the energy distribution, and as a consequence temperature hike is witnessed.

Prandtl number effect on temperature is depicted in Figure 13, which indicates a major reduction in temperature profile with Pr, which is conventional. The Prandtl number represents the momentum diffusivity to thermal diffusivity ratio and a higher Prandtl number corresponds to smaller thermal diffusivity. Here to get a clear understanding of the influence of the Prandtl number, its values are considered as 1.0, 2.0, 3.0, 4.0. So, this is observed that as the Prandtl number increases, the thermal boundary layer becomes thinner. Hence, the Prandtl number can be used to speed up the cooling rate in a conducting flow.

Figure 14 illustrates the effect of A_2 and n on the skin-friction coefficient $Re^{1/2}C_f$, which reflects that $Re^{1/2}C_f$ (related to surface drag force) shows an increasing trend with a decrement of A_2 and opposite trend for n increment. The effect of the non-linear mixed convention is

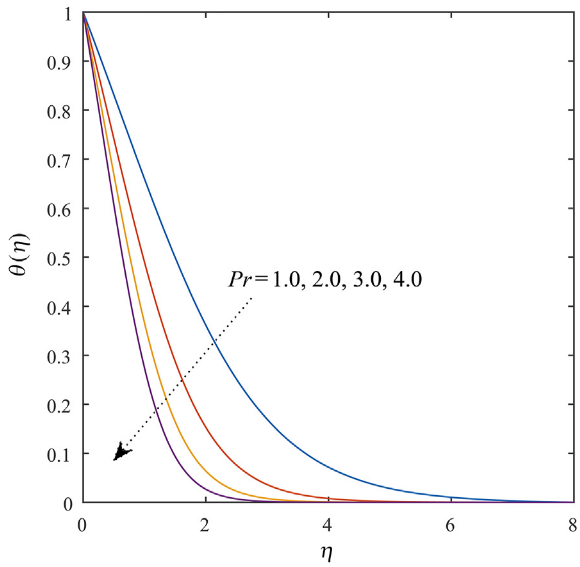

Figure 13 Effect of Pr on $\theta(\eta)$.

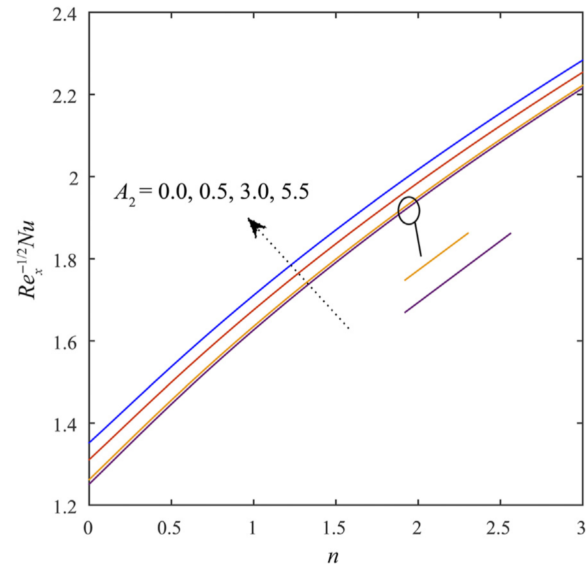

Figure 15 Influences of A_2 and n on $Re^{-1/2}Nu$.

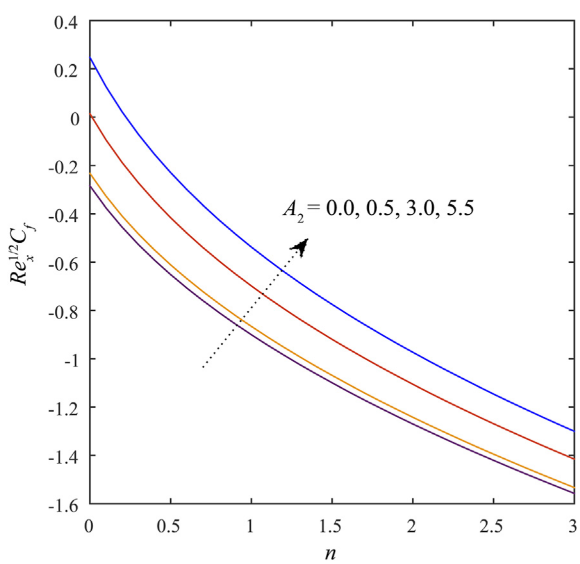

Figure 14 Influences of A_2 and n on $Re^{1/2}C_f$.

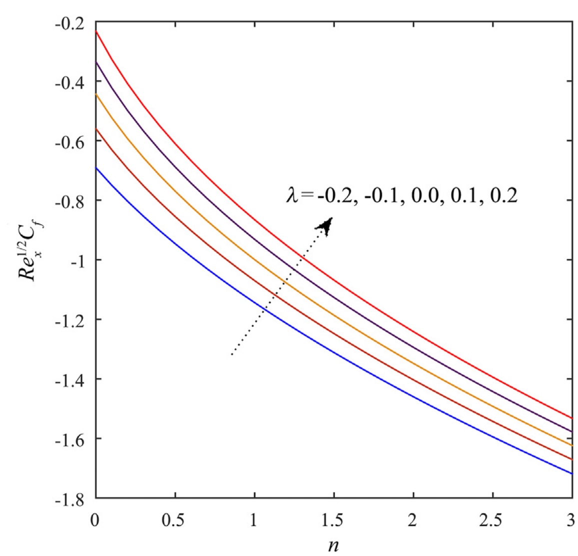

Figure 16 Influences of λ and n on $Re^{1/2}C_f$.

overshadowed by non-linear stretching. So, due to the non-linear aspect of the buoyancy effect, the drag force diminishes and non-linear variation in stretching velocity along the sheet causes higher drag towards the neighbouring fluid layer. Figure 15 depicts the influence of A_2 and n on the Nusselt number. It is quite clear that the Nusselt number $Re^{-1/2}Nu$ (related to heat transfer rate) increases with both A_2 and n and it agrees with the classical concept. The effect of λ on $Re^{1/2}C_f$ for variation in n is demonstrated in Figure 16. The magnitude of $Re^{1/2}C_f$, i.e., surface-drag falls for assisting flow ($\lambda > 0$) and rises for opposing flow ($\lambda < 0$). This happens due to opposite types of forces in assisting and opposing flows. Figure 17 shows the effect of buoyancy parameter λ on $Re^{-1/2}Nu$ with n, and it reflects that as λ increases, heat transfer rate increases. Obviously, the occurrence of the usual linear buoyancy force produces the cooling rate hike. Figure 18 depicts the changes in $Re^{1/2}C_f$ due to variations in θ_w and Nr. The surface-drag magnitude exhibits a decreasing behaviour as the value of the temperature ratio parameter θ_w increases. Similarly, increasing the non-linear radiation parameter Nr generates a considerable reduction in the magnitude of surface-drag force (i.e., skin-friction coefficient), and the impact of Nr is more profound when the temperature ratio parameter is large. Non-linear radiation via non-linear mixed convection acts behind this reduction. Figure 19 depicts the influences of θ_w, Pr, Nr on the Nusselt number. It is detected that with augmentations of θ_w, Pr and Nr, the heat transfer rate $(Re^{-1/2}Nu)$ increases. Physically, it is expected, because the

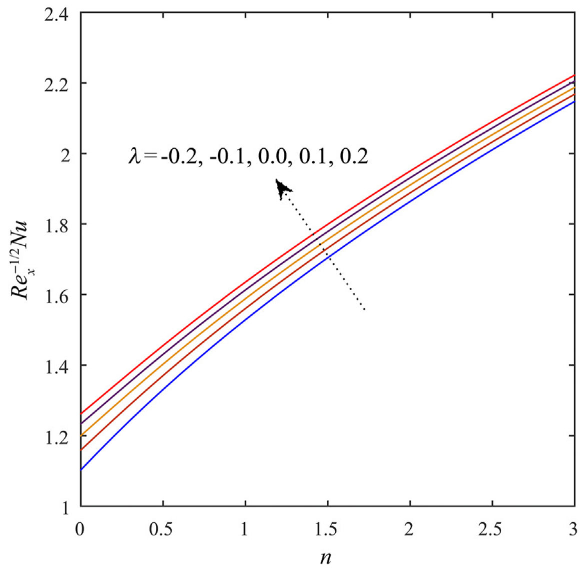

Figure 17 Influences of λ and n on $Re^{-1/2}Nu$.

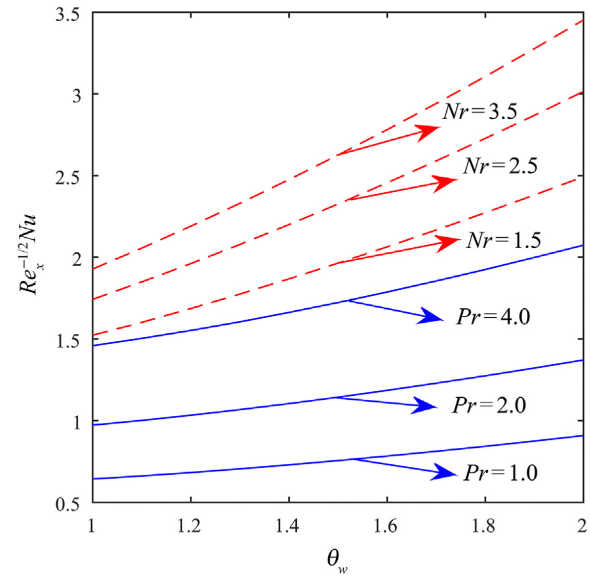

Figure 19 Influences of θ_w, Pr and Nr on $Re^{-1/2}Nu$.

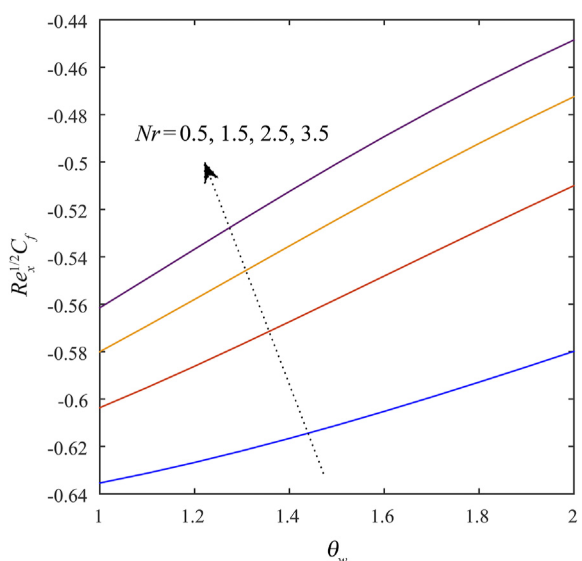

Figure 18 Influences of θ_w and Nr on $Re^{1/2}C_f$.

Table 4 The computed values of local skin-friction and local Nusselt number for different parameters.

n	A_2	λ	Nr	θ_w	$Re^{1/2}C_f$	$Re^{-1/2}Nu$
0.5	0.5	0.2	0.5	1.5	−0.6110476	1.4556631
1					−0.8660896	1.6352450
2					−1.2418499	1.9501163
3					−1.5330613	2.2222129
0.5	0.0				−0.6514050	1.4460329
	0.5				−0.6110476	1.4556631
	3.0				−0.4158493	1.4993092
	5.5				−0.2295329	1.5372504
	0.5	−0.2			−0.9468167	1.3310393
		−0.1			−0.8556611	1.3706172
		0.0			−0.7704260	1.4029715
		0.1			−0.6892178	1.4308703
		0.2			−0.6110476	1.4556631
		0.2	0.5		−0.6110476	1.4556631
			1.5		−0.5577781	1.9640688
			2.5		−0.5242500	2.3258711
			3.5		−0.5006402	2.6256642
			0.5	1.1	−0.6313104	1.2722089
				1.3	−0.6218613	1.3572606
				1.5	−0.6110476	1.4556631
				1.8	−0.5928748	1.6243590

non-linearity in the consideration of thermal radiation acts in favour of quicker cooling, i.e., higher heat transfer rate from the surface. The above-mentioned effects on $Re^{1/2}C_f$ and $Re^{-1/2}Nu$ of several parameters are also tabulated in Table 4.

5. Final remarks

An original investigation on influences of non-linear mixed convection and non-linear thermal radiation on Newtonian flow on a non-linearly stretching vertical surface is conducted and the following conclusions are summarized from a thorough analysis of interactive effects:

- The non-linear convection parameter A_2 has opposite effects on velocity, i.e., near the surface of the sheet, velocity increases, and away from the sheet, velocity decreases.
- With non-linearity in mixed convection character, the temperature drop is witnessed.
- Increase of non-linear stretching parameter n leads to a decrease in dimensionless velocity, but a contrary result for temperature is detected.
- With the growths of Nr and θ_w, the velocity and temperature also grows.

- The magnitude of surface-drag force reduces with A_2, Nr and θ_w and it rises with n.
- If A_2 changes from 0 to 0.5 then the magnitude of skin-friction coefficient diminishes upto 6.2% (approx.), whereas the variation in the values of n from 1 to 2 produces 43.4% (approx.) hike. Similarly, if Nr increases to 1.5 from 0.5, then $Re^{1/2}C_f$ shows 8.7% reduction.
- Nusselt number (i.e., heat transfer rate) increases as the value of A_2, n, Nr and θ_w.
- The increment of n from 1 to 2 causes 19.3% (approx.) upsurge in $Re^{-1/2}Nu$ and 33.2% (approx.) improvement $Re^{-1/2}Nu$ observed when Nr increases to 1.5 from 0.5.

Acknowledgements

The work of A.K. Pandey is funded by CSIR [09/013(0742)/2018-EMR-I] and the research of A.K. Gautam is supported by UGC [1220/(CSIR-UGC NET DEC. 2016)]. The authors are thankful to the anonymous reviewers for their precious comments.

References

[1] F. Mabood, W.A. Khan, A.I. Ismail, Analytical solution for radiation effects on heat transfer in Blasius flow, International Journal of Modern Engineering Sciences 2 (2013) 63−72.
[2] W.A. Khan, M.J. Uddin, A.I. Ismail, Effects of radiation on Blasius slip flow of oxide nanofluids with Merkin boundary condition, Proc. Inst. Mech. Eng. - Part N J. Nanoeng. Nanosyst. 227 (2012) 3−9.
[3] T. Hayat, T. Muhammad, A. Alsaedi, M.S. Alhuthali, Magnetohydrodynamic three-dimensional flow of viscoelastic nanofluid in the presence of nonlinear thermal radiation, J. Magn. Magn Mater. 385 (2015) 222−229.
[4] S.A. Shehzad, T. Hayat, A. Alsaedi, M.A. Obid, Nonlinear thermal radiation in three-dimensional flow of Jeffrey nanofluid: a model for solar energy, Appl. Math. Comput. 248 (2014) 273−286.
[5] G.K. Kumar, B.J. Gireesha, S. Manjunatha, N.G. Rudraswamy, Effect of nonlinear thermal radiation on double-diffusive mixed convection boundary layer flow of viscoelastic nanofluid over a stretching sheet, Int. J. Mech. Mater. Eng. 12 (2017) 18.
[6] I.L. Animasaun, C.S.K. Raju, N. Sandeep, Unequal diffusivities case of homogeneous−heterogeneous reactions within viscoelastic fluid flow in the presence of induced magnetic-field and nonlinear thermal radiation, Alex. Eng. J. 55 (2) (2016) 1595−1606.
[7] T. Hayat, M. Imtiaz, A. Alsaedi, M.A. Kutbi, MHD three-dimensional flow of nanofluid with velocity slip and nonlinear thermal radiation, J. Magn. Magn Mater. 396 (2015) 31−37.
[8] M.M. Nandeppanavar, M.C. Kemparaju, N. Raveendra, Effect of nonlinear thermal radiation on the stagnation point flow of double diffusive free convection due to moving vertical plate, J. Eng. Des. Technol. (2021), https://doi.org/10.1108/JEDT-10-2020-0430.
[9] M. Ahmad, I. Ahmad, M. Sajid, Magnetohydrodynamic time dependent three-dimensional flow of Maxwell fluid over a stretching surface through porous space with variable thermal conditions, J. Braz. Soc. Mech. Sci. Eng. 38 (2016) 1767−1778.
[10] B. Mahanthesh, B.J. Gireesha, I.L. Animasaun, Exploration of nonlinear thermal radiation and suspended nanoparticles effects on mixed convection boundary layer flow of nanoliquids on a melting vertical surface, Journal of Nanofluids 7 (5) (2018) 833−843.
[11] O.K. Koriko, I.L. Animasaun, A.J. Omowaye, T. Oreyeni, The combined influence of nonlinear thermal radiation and thermal stratification on the dynamics of micropolar fluid along a vertical surface, Multidiscip. Model. Mater. Struct. 15 (1) (2019) 133−155.
[12] M.I. Khan, H. Waqas, S.U. Khan, M. Imran, Y.-M. Chu, A. Abbasi, S. Kadry, Slip flow of micropolar nanofluid over a porous rotating disk with motile microorganisms, nonlinear thermal radiation and activation energy, Int. Commun. Heat Mass Tran. 122 (2021) 105161.
[13] Y.Q. Song, S.A. Khan, M. Imran, H. Waqas, S.U. Khan, M.I. Khan, S. Qayyum, Y.-M. Chu, Applications of modified Darcy law and nonlinear thermal radiation in bioconvection flow of micropolar nanofluid over an off centered rotating disk, Alex. Eng. J. 60 (2021) 4607−4618.
[14] H. Waqas, S.A. Khan, S.U. Khan, M.I. Khan, S. Kadry, Y.-M. Chu, Falkner-Skan time-dependent bioconvrction flow of cross nanofluid with nonlinear thermal radiation, activation energy and melting process, Int. Commun. Heat Mass Tran. 120 (2021) 105028.
[15] M. Bilal, M. Ramzan, Y. Mehmood, M. Kbiri Alaoui, R. Chinram, An entropy optimization study of non-Darcian magnetohydrodynamic Williamson nanofluid with nonlinear thermal radiation over a stratified sheet, Proc. IME E J. Process Mech. Eng. 235 (2021) 1883−1894.
[16] S.L. Goren, On free convection in water at 4°C, Chem. Eng. Sci. 21 (1966) 515−518.
[17] B. Ali, A. Shafiq, A. Manan, A. Wakif, S. Hussain, Bioconvection: significance of mixed convection and MHD on dynamics of Casson nanofluid in the stagnation point of rotating sphere via finite element simulation, Math. Comput. Simulat. 194 (2022) 254−268.
[18] B. Mahanthesh, B.J. Gireesha, G.T. Thammanna, S.A. Shehzad, F.M. Abbasi, R.S.R. Gorla, Nonlinear convection in nano Maxwell fluid with nonlinear thermal radiation: a three-dimensional study, Alex. Eng. J. 57 (3) (2018) 1927−1935.
[19] T. Hayat, S. Qayyum, A. Alsaedi, B. Ahmad, Modern aspects of nonlinear convection and magnetic field in flow of thixotropic nanofluid over a nonlinear stretching sheet with variable thickness, Phys. B Condens. Matter 537 (2018) 267−276.
[20] M. Waqas, M.I. Khan, T. Hayat, A. Alsaedi, Effect of nonlinear convection on stratified flow of third grade fluid with revised Fourier-Fick relations, Commun. Theor. Phys. 70 (7) (2018) 25−30.
[21] B.J. Gireesha, P.B. Sampath Kumar, B. Mahanthesh, S.A. Shehzad, F.M. Abbasi, Nonlinear gravitational and radiation aspects in nanoliquid with exponential space dependent heat source and variable viscosity, Microgravity Sci. Technol. 30 (3) (2018) 257−264.
[22] M. Bandaru, M.M. Rashidi, H. Raju, Influence of non-linear convection and thermophoresis on heat and mass transfer from a rotating cone to fluid flow in porous medium, Therm. Sci. 21 (2017) 2781−2793.
[23] I. Uddin, R. Akhtar, M.A. Rehman Khan, Z. Zhiyu, S. Islam, M. Shoaib, M.A. Zahoor Raja, Numerical treatment for fluidic system of activation energy with non-linear mixed convective and radiative flow of magneto nanomaterials with Navier's velocity slip, AIP Adv. 9 (2019) 055210.
[24] B. Mahanthesh, I.L. Animasaun, M. Rahimi-Gorji, I.M. Alarifi, Quadratic convective transport of dusty Casson and dusty Carreau fluids past a stretched surface with nonlinear thermal radiation, convective condition and non-uniform heat source/sink, Phys. Stat. Mech. Appl. 535 (2019) 122471.
[25] T. Kunnegowda, B. Mahanthesh, G. Lorenzini, I.L. Animasaun, Significance of induced magnetic field and exponential space dependent heat source on quadratic convective flow of Casson fluid in a micro-channel via HPM, Mathematical Modelling of Engineering Problems 6 (3) (2019) 369−384.
[26] A. Alsaedi, T. Hayat, S. Qayyum, R. Yaqoob, Eyring−Powell nanofluid flow with nonlinear mixed convection: entropy generation minimization, Comput. Methods Progr. Biomed. 186 (2020) 105183.
[27] K. Hong, R. Alizadeh, M.V. Ardalan, A. Nourbakhsh, N. Karimi, Y. Yang, Q. Xiong, Numerical study of nonlinear mixed convection inside stagnation point flow over surface reactive cylinder embedded in porous media, J. Therm. Anal. Calorim. 141 (2020) 1889−1903.
[28] S. Rajput, A.K. Verma, K. Bhattacharyya, A.J. Chamkha, Unsteady nonlinear mixed convective flow of nanofluid over a wedge: Buongiorno model, Waves in Random and Complex Media (2021), https://doi.org/10.1080/17455030.2021.1987586.
[29] P.M. Patil, H.F. Shankar, P.S. Hiremath, E. Momoniat, Nonlinear mixed convective nanofluid flow about a rough sphere with the diffusion of liquid hydrogen, Alex. Eng. J. 60 (2021) 1043−1053.

[30] S. Aziz, N. Ali, I. Ahmad, U.F. Alqsair, S.U. Khan, Contributions of nonlinear mixed convection for enhancing the thermal efficiency of Eyring-Powell nanoparticles for periodically accelerated bidirectional flow, Waves in Random and Complex Media (2021), https://doi.org/10.1080/17455030.2021.2022812.

[31] B. Mahanthesh, C. Srinivas Reddy, N. Srikantha, G. Lorenzini, Entropy generation analysis of radiative heat transfer in Williamson fluid flowing in a microchannel with nonlinear mixed convection and Joule heating, Proc. IME E J. Process Mech. Eng. (2022), https://doi.org/10.1177/09544089221074846.

[32] A. Kumar, R.K. Ray, M.A. Sheremet, Entropy generation on double-diffusive MHD slip flow of nanofluid over a rotating disk with nonlinear mixed convection and Arrhenius activation energy, Indian J. Phys. 96 (2022) 525−541.

[33] R. Cortell, Viscous flow and heat transfer over a nonlinear stretching sheet, Appl. Math. Comput. 184 (2007) 864−873.

[34] P. Rana, R. Bhargava, Flow and heat transfer of a nanofluid over a nonlinearly stretching sheet: a numerical study, Commun. Nonlinear Sci. Numer. Simulat. 17 (2012) 212−226.

[35] D. Pal, G. Mandal, Hydromagnetic convective-radiative boundary layer flow of nanofluids induced by a non-linear vertical stretching/shrinking sheet with viscous-Ohmic dissipation, Powder Technol. 279 (2015) 61−74.

[36] K. Gangadhar, R.E. Nayak, M.V.S. Rao, Buoyancy effect on mixed convection boundary layer flow of Casson fluid over a non-linear stretched sheet using the spectral relaxation method, Int. J. Ambient Energy (2020), https://doi.org/10.1080/01430750.2020.1722963.

[37] M. Turkyilmazoglu, Multiple analytic solutions of heat and mass transfer of magnetohydrodynamic slip flow for two types of viscoelastic fluids over a stretching surface, ASME Journal of Heat Transfer 134 (7) (2012) 071701.

[38] O.J. Fenuga, A.R. Hassan, P.O. Olanrewaju, Effects of radiation and Eckert number on MHD flow with heat transfer rate near a stagnation point over a non-linear vertical stretching sheet, Int. J. Appl. Mech. Eng. 25 (2020) 27−36.

[39] M. Turkyilmazoglu, Extending the traditional Jeffery-Hamel flow to stretchable convergent/divergent channels, Comput. Fluid 100 (2014) 196−203.

[40] K.V. Prasad, S.R. Santhi, P.S. Datti, Non-Newtonian power-law fluid flow and heat transfer over a non-linearly stretching surface, Appl. Math. 3 (2012) 425−435.

[41] M.A.A. Mahmoud, A.M. Megahed, Non-uniform heat generation effect on heat transfer of a non-newtonian power-law fluid over a non-linearly stretching sheet, Meccanica 47 (2012) 1131−1139.

[42] S. Jothimani, T. Vidhya, Non-Newtonian fluid flow and heat transfer over a non -linearly stretching surface along with porous plate in porous medium, Int. J. Eng. Res. Afr. 8 (2014) 5−13.

[43] M. Khan, Hashim, Boundary layer flow and heat transfer to Carreau fluid over a nonlinear stretching sheet, AIP Adv. 5 (2015) 107203.

[44] M. Hamid, M. Usman, Z.H. Khan, R.U. Haq, W. Wang, Numerical study of unsteady MHD flow of Williamson nanofluid in a permeable channel with heat source/sink and thermal radiation, Eur. J. 133 (2018) 527.

[45] T. Hayat, I. Ullah, A. Alsaedi, B. Ahamad, Simultaneous effects of non-linear mixed convection and radiative flow due to Riga-plate with double stratification, AMSE Journal of Heat Transfer 140 (2018) 102008.

[46] T. Vijaya Laxmi, B. Shankar, Effect of non-linear thermal radiation on boundary layer flow of viscous fluid over non-linear stretching sheet with injection/suction, J. Appl. Math. Phys. 4 (2016) 307−319.

[47] M.H. Matin, M. Dehsara, A. Abbassi, Mixed convection MHD flow of nanofluid over a non-linear stretching sheet with effects of viscous dissipation and variable magnetic field, Mechanika 18 (4) (2012) 415−423.

[48] L.F. Shampine, I. Gladwell, S. Thompson, Solving ODEs with MATLAB, Cambridge University Press, 2003.

[49] M. Usman, M. Hamid, T. Zubair, R.U. Haq, W. Wang, Operational-matrix-based algorithm for differential equations of fractional order with Dirichlet boundary conditions, The European Physical Journal - Plus 134 (2019) 279.

[50] M. Hamid, M. Usman, R.U. Haq, W. Wang, A Chelyshkov polynomial based algorithm to analyze the transport dynamics and anomalous diffusion in fractional model, Phys. Stat. Mech. Appl. 551 (2020) 124227.

[51] M. Hamid, M. Usman, W. Wang, Z. Tian, A stable computational approach to analyse semi-relativistic behavior of fractional evolutionary problems, Numer. Methods Part. Differ. Equ. 38 (2022) 122−136.